Polarization Rotation in a Second Harmonic Reflection Experiment from an Isotropic Surface of Chiral Tröger Base

F. Hache,*,† T. Boulesteix,† M. C. Schanne-Klein,† M. Alexandre,‡ G. Lemercier,‡ and C. Andraud‡

Laboratoire d'Optique et Biosciences, CNRS-INSERM, Ecole Polytechnique, 91128 Palaiseau Cedex, France, and Ecole Normale Supérieure de Lyon, STIM, 69364 Lyon Cedex 07, France

Received: January 27, 2003; In Final Form: April 8, 2003

Polarization rotation in second harmonic reflection (ORD-SHR) is carefully investigated. After emphasizing the relevance of this technique for characterization of chiral molecules the optical activity of which arises from electric contributions, we bring an experimental demonstration with a specially synthesized acridine-substituted Tröger base, which displays very strong rotations. Measurements of this rotation for wavelengths spanning the absorption spectrum are satisfactorily reproduced by a model based on coupled, anharmonic oscillators.

I. Introduction

Second harmonic reflection (SHR) from molecules deposited on a surface has been shown for a decade to be a very sensitive probe of the molecular chirality. Pioneering work by Hicks and co-workers[1] and Persoons and co-workers,[2] followed by many others,[3−6] has allowed the unique properties of these measurements to be widely studied, and many chiral surfaces have already been characterized in this way. However, new information on the chirality of the individual molecules is not always obtained directly from these experiments: for example, it is well-known that an asymmetric arrangement of achiral molecules can give rise to a chiral response in SHR.[7,8] One must therefore be very cautious when using such SHR results to study the chirality of molecules. An unquestionable way to avoid these problems is to do the experiments for the two enantiomeric forms of the molecule and to make sure that they give opposite results. If such conditions are fulfilled, three particular experiments prove to be very powerful to study the molecular chirality. First, one can send a *p*-polarized fundamental beam and measure the rotation of the second harmonic (SH) polarization (ORD-SHR): any rotation is a signature of the chirality; it is a consequence of the breakdown of the symmetry of the experiment due to the lack of symmetry of the individual molecules. Second, one can measure the SH intensity for a right- and a left-circularly polarized fundamental beam. Any difference in these two SH signals is also a consequence of the chirality of the molecules (CD-SHR). Third, one can do the same measurements for a fundamental beam polarized at $+45°$ or $-45°$ of the *p*-direction. Here again, the SH signals will be different only for chiral molecules (LD-SHR). The last two techniques can be refined by continuously changing the (elliptical or linear) polarization of the fundamental beam with a Babinet−Soleil compensator and measuring the SH intensity. Fitting of these curves allows the determination of a host of information on the second-order response of the molecules.[3,9,10]

In this article, we are primarily interested in the first technique, ORD-SHR. This technique has the advantage of being straightforward and of mimicking the frequently used linear ORD technique, which is a standard one in the characterization of chiral molecules. First evidence of ORD-SHR was given in ref 11 in which a polarization rotation of 17° was measured from SHR on a binaphthol surface. Similar experiments on a chiral dye[3] and on a sugar[5] have also been reported. However, it has soon appeared that the uniqueness of this technique was doubtful to characterize chiral molecules and that some chiral molecules could display strong CD-SHR without any ORD-SHR.[12] The ambiguity was lifted when one realized that this technique was very dependent on the microscopic origin of the optical activity in the chiral molecules. Optical activity can arise from several mechanisms:[13,14] it can be of dipolar electric, dipolar magnetic, or quadrupolar electric origin. However, it was shown that ORD-SHR was effective only for the first case,[14] and it is the purpose of this paper to examine this point in greater detail. In the next section, we investigate the ORD-SHR from a theoretical point of view and clearly recover the above-mentioned selectivity of ORD-SHR for molecules displaying dipolar electric chirality. We then present experimental results obtained with the two enantiomers of a specially designed acridine-substituted Tröger base, which displays ORD-SHR as strong as $\pm 66°$.[15] The frequency dependence of this ORD-SHR is studied across the absorption band of the molecule. In the final section, we develop a model calculation based on coupled, anharmonic oscillators, which allows us to understand the measured dependence.

II. Theory of ORD-SHR

Thorough theoretical treatment of SHR from a chiral surface can be found in refs 2 and 3. Here, we briefly outline the theory necessary for ORD-SHR. An isotropic surface of chiral molecules can be described, as far as SHR is concerned, in terms of surface second-order susceptibilities. However, optical activity being a nonlocal phenomenon, one must introduce not only the "electric" susceptibility, χ^{eee}, but also two "magnetic" ones, χ^{mee} and χ^{eem}:[2] Following the usual way of writing, we cast the electric dipolar contributions under a generic "electric" term

* To whom correspondence should be addressed. E-mail: francois.hache@polytechnique.fr.
† Ecole Polytechnique.
‡ Ecole Normale Supérieure de Lyon.

10.1021/jp034216+ CCC: $25.00
Published on Web 05/02/2003

and the magnetic dipolar and electric quadrupolar contributions under a generic "magnetic" term. In ref 14, we have indeed theoretically shown that SHR experiments do not allow one to separate the latter two contributions. Each susceptibility tensor has achiral components, which do not vanish in general, whatever the molecule, and chiral ones, which are nonzero only for chiral molecules. ORD-SHG experiments consist in sending a *p*-polarized fundamental beam at an angle θ of the surface normal and measuring the polarization of the SH beam. Following the notation of ref 2, we write

$$E_{p,s}(2\omega) \propto f_{p,s}E_p^{\,2}(\omega) \tag{2.1}$$

The two coefficients f_p and f_s have the remarkable property that they sort out achiral and chiral components. The expression of f_p only involves *achiral* components, whereas the expression of f_s only involves *chiral* ones:[2]

$$f_p = \sin\theta(-2\chi_{xyz}^{eee}\cos\theta - \chi_{xzx}^{eem} + \chi_{zzz}^{mee}\sin^2\theta + \chi_{zxx}^{mee}\cos^2\theta - 2\chi_{xxz}^{mee}\cos^2\theta) \tag{2.2}$$

$$f_s = \sin\theta(\chi_{zzz}^{eee}\sin^2\theta + \chi_{zxx}^{eee}\cos^2\theta - 2\chi_{xzz}^{eee}\cos^2\theta - \chi_{zxy}^{eem}\cos\theta + \chi_{xzy}^{eem}\cos\theta + 2\chi_{xyz}^{mee}\cos\theta) \tag{2.3}$$

Note that in these formulas the Fresnel coefficients have been neglected for the sake of readability. Complete expressions can be found in ref 3. From eq 2.1, one can calculate the SH signal through an analyzer and deduce the rotation angle of the SH polarization. Let us call δ the angle between the analyzer and the *p*-direction. The transmitted SH signal is

$$S = |E_p(2\omega)\cos\delta + E_s(2\omega)\sin\delta|^2 \tag{2.4}$$

$$= (|f_p|^2\cos^2\delta + |f_s|^2\sin^2\delta + 2(f_p'f_s' + f_p''f_s'')\sin\delta\cos\delta)|E_p(\omega)|^2 \tag{2.5}$$

where the $'$ and $''$ correspond to the real and imaginary part of the coefficients. The rotation angle is defined as the analyzer angle, δ_m, for which S is maximum. Differentiating the above expression with respect to δ leads to

$$\tan 2\delta_m = \frac{2(f_p'f_s' + f_p''f_s'')}{|f_p|^2 - |f_s|^2} \tag{2.6}$$

This expression is however not enough to determine unambiguously the rotation angle because it gives two angles (separated by π), which correspond to a minimum and a maximum of S. One must therefore check with the second-order derivative that S is maximum, and one obtains the following condition:

$$\text{if} \quad |f_p|^2 - |f_s|^2 > 0, \quad \text{then} \quad \delta_m = \frac{1}{2}\arctan\frac{2(f_p'f_s' + f_p''f_s'')}{|f_p|^2 - |f_s|^2} \tag{2.7}$$

$$\text{if} \quad |f_p|^2 - |f_s|^2 < 0, \quad \text{then} \quad \delta_m = \frac{1}{2}\arctan\frac{2(f_p'f_s' + f_p''f_s'')}{|f_p|^2 - |f_s|^2} + \pi \tag{2.8}$$

This careful analysis will prove to be useful in section IV.

Equations 2.7 and 2.8 allow us to readily retrieve fundamental aspects of ORD-SHR. First of all, if the molecules are not chiral, we have $f_s = 0$, and it is straightforward to check that there is no SH polarization rotation ($\delta_m = 0$), as expected. Second, one can notice that the numerators in eqs 2.7 and 2.8 imply a mixing of *real* and *imaginary* parts. This proves to have important consequences on the influence of the microscopic origin of optical activity on the relevance of ORD-SHR. Indeed, electric and magnetic susceptibilities experience a phase difference of $\pi/2$. This can be traced back to the quantum expressions, which involve three electric dipole moments in the former case and two electric dipole moments plus one magnetic one in the latter, resulting in this phase difference.[2] This is rigorously true off-resonance where the electric susceptibility is real whereas the magnetic ones are purely imaginary, but it is also true on-resonance as soon as the electric and magnetic contributions come from the same transitions, as is usually the case in chiral molecules. Let us now come back to eqs 2.7 and 2.8. In most cases (and in all of the experimental cases), the achiral susceptibility is dominated by the electric contribution. If the microscopic origin of the optical activity is *electric*, it means that f_s is in phase with f_p, in which case, δ_m is nonzero. On the contrary, if the origin of the optical activity is *magnetic*, f_s is in quadrature with f_p and δ_m vanishes. This observation allows the observed nonuniversality of ORD-SHR to be fully understood: ORD-SHR will be sensitive to optical activity arising only from electric effects and not from magnetic effects.[12]

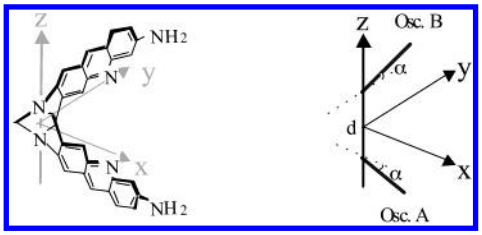

Figure 1. Chemical structure of the acridine-substituted Tröger base. The corresponding coupled-oscillator model is also shown.

III. Experiment

In this section, we present experiments aimed at demonstrating the relevance of the previous statements for obtaining a large ORD-SHR effect. The point is to design a chiral molecule suitable for surface second harmonic generation, of which the optical activity is primarily of electric origin. The best choice to satisfy this last point is to investigate molecules displaying an excitonic coupling, that is, molecules composed of two oscillators arranged in a nonsymmetrical manner. The coupling between the two oscillators, through electrostatic interaction, for example, leads to optical activity.[16] On the other hand, to get measurable SH signals, it is important that the molecules be highly polarizable with a well-defined direction of polarization. At last, we must have molecules the absorption spectra of which are in concordance with the available laser wavelengths. From a practical point of view, it is also important that the molecules be soluble and chemically stable. Considering all of the aforementioned requirements, we have fixed our choice on an acridine-substituted Tröger base. The molecule structure is sketched in Figure 1. The usual Tröger base (methanodibenzo-1,5-diazocine) is substituted with acridines on both sides of the diazocine bridge. It meets all of the needed specifications: the two acridines form the two noncollinear oscillators and the delocalized electrons along the acridine structures ensure a good optical nonlinear response. Furthermore, this molecule seems to be apt to fix on a silica substrate owing to its amine terminal groups, which is a preliminary requirement for any SHR experiment to be performed.

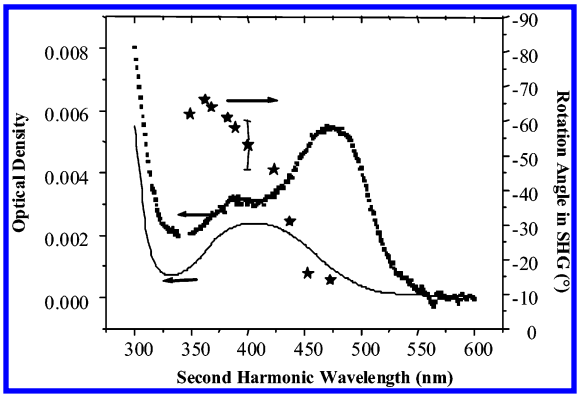

Figure 2. Optical density of (■) a film of the (−) enantiomer relative to the bare fused silica substrate and (—) the ethanolic solution of the (−) enantiomer (divided by 300) and (★) rotation angle of the SHG signal measured on the thin film.

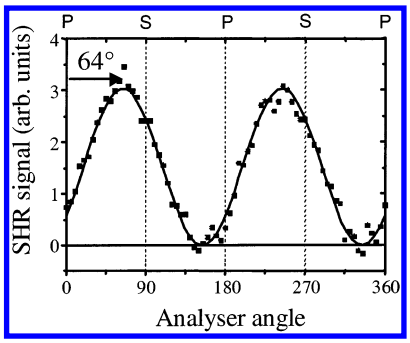

Figure 3. Second harmonic signal measured by reflection of a *p*-polarized fundamental beam on a thin film of the Tröger base as a function of the analyzer angle.

Synthesis of this molecule and preparation of the samples have been presented in ref 17. The absorption spectra of the molecule in ethanol (7×10^{-4} M) and of the molecules deposited on a silica substrate by a dipping procedure are shown in Figure 2. The former presents a band around 400 nm associated with a single-signed circular dichroic structure (not shown, see ref 17). The latter displays the same band but with another red-shifted band. The origin of this band is not clear, but it does not seem to play a role in the SHR experiment. From the optical density of our sample, we can deduce a surface coverage on the order of 10^{14} molecules/cm^2, indicating that each molecule has an average surface of 1 nm^2, compatible with a monolayer of not too densely packed molecules. We have checked that the surface is isotropic by performing the experiments for several positions of the sample without noticing any difference.

The SHR setup is described in ref 12. It is based on an 82 MHz titanium−sapphire laser tunable in the 700−1000 nm range. Once frequency-doubled by the SHR process, this tuning range spans the absorption structure of our sample. The weak SH signal is detected by a photon-counting photomultiplier tube coupled to a lock-in amplifier locked on a 160 Hz optical chopper placed on the fundamental beam. For the ORD-SHR experiment, the polarization of the impinging fundamental beam is fixed to *p* by a Glan prism. The SH signal polarization is measured after rotation of another Glan prism. Typical results of such an experiment are displayed in Figure 3. One clearly sees that the SH beam is not *p*-polarized but that there is a rotation of 64° of the polarization. Note also that the SH beam is linearly polarized, as can be inferred from the fact that the signal drops to 0 for particular position of the analyzer. This very strong rotation was measured for a fundamental wavelength

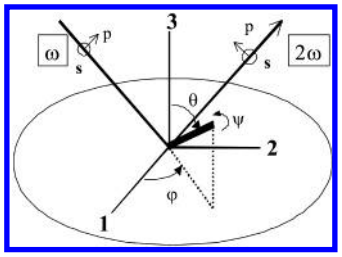

Figure 4. Geometry of the SHR experiment. The thick bar represents a molecule referenced by the Euler angles.

of 740 nm, corresponding to a SH wavelength (370 nm) on resonance with the absorption band. To better understand the influence of resonance on the rotation angle, we have performed the ORD-SHR measurements as a function of the wavelength. The SH wavelength goes from 475 to 350 nm and spans all of the absorption structure. The measured rotation angles are displayed in Figure 2. One can observe a continuous increase of the angle from 10° to 66°. A point worth noting is that there is no special feature when the SH wavelength crosses the maximum of the absorption structure. We will come back to this point in the next section in which we want to model the behavior of the SH rotation angle as a function of the wavelength. Note that such large rotation angles have never been obtained before, to the best of our knowledge, emphasizing the relevance of molecular engineering.

We have carried out all of these measurements for the two enantiomers. In every case, we obtain perfectly symmetrical results, the rotation angle changing sign but not magnitude for the two species. We have also checked that there was no SHR optical activity for a racemic mixture. This feature gives us further confidence that the molecules are isotropically distributed over the surface and that our measurements are free from artifacts originating in the alignment of the molecules on the surface[7] and only probe the chirality of the molecules.

IV. Model Calculation of the ORD-SHR

The principle of such a calculation of the SH electric field radiated by a surface of chiral molecules has been thoroughly discussed in ref 14, in which all of the electric and magnetic contributions to the SH signal were taken into account and in which the fundamental electric field had no privileged polarization. These two constraints are relaxed in our present calculation. First, considering the structure of the molecule, we can concentrate on the electric contributions. It is well-known that magnetic parts are negligible compared to electric ones as soon as these latter do not vanish. This is true for the achiral contribution, but it is not so obvious as far as the chiral components are concerned. This hypothesis is however supported by the experimental results presented in Figure 3. Indeed, the fact that the SH beam remains linearly polarized implies that f_p and f_s are in phase, which is possible only if the chiral magnetic terms are negligible compared to the electric ones. Second, as we are interested here in an ORD-SHR experiment, we can suppose that the fundamental beam is *p*-polarized.

We recall now briefly the principle of the calculation. Let us call (1, 2, 3) the laboratory frame attached to the substrate surface and (*x*, *y*, *z*) the molecular one. One passes from the latter to the former by three rotations associated with the molecule Euler angles θ, φ, and ψ (see Figure 4). The first step is the calculation of the hyperpolarizability, β, of the molecule in the (*x*, *y*, *z*) system. This is the heart of the problem and necessitates the introduction of a model that we will discuss

in the next subsection. Then, one obtains the surface second-order susceptibility, $\chi^{(2)}$, by averaging the β's over the molecule distribution. Because we experimentally deal with an isotropic surface, it amounts to averaging over a random distribution for φ. We do not make any hypothesis at this point on the other two angles θ and ψ. Once the nonlinear susceptibility is known, it is possible to calculate the radiated SH electric field and henceforth to obtain the f_p and f_s parameters and to apply eqs 2.7 and 2.8 to obtain the SH rotation angle. We come now to the model used to calculate the hyperpolarizability of the Tröger molecules.

A. Calculation of the Hyperpolarizability: The Kuhn Model. As already stated, optical activity in the Tröger base arises from the coupling of two electric dipoles arranged in a noncentrosymmetrical manner, and the molecule therefore clearly pertains to the Kuhn model.[18] Evidence for the adequation of this model can be seen in Figure 1 in which the molecular structure is displayed together with the relevant Kuhn model. Calling z the axis passing through the two central nitrogen atoms, one can model the two acridines by two oscillators A and B lying in the xz and yz planes, respectively, and making an angle α with the x and y axes, as in our previous calculation.[14] This model has been successfully utilized to perform a quantum calculation of sum-frequency generation in a binaphthol solution.[19] In this article, we stick to a classical calculation, which provides a more direct perception of the problem.

The two oscillators have the same frequency, ω_0, and the same friction coefficient, γ, and are coupled through dipole−dipole interaction with a coupling parameter, κ. This system is excited by a monochromatic electric field, E. Let us call a and b the elongations of the two oscillators compared to their equilibrium positions. The equations of motion at the first order in the fundamental electric field are

$$D_\omega a^{(1)} + \kappa b^{(1)} = \frac{-e}{m}[E_x \cos\alpha - E_z \sin\alpha]$$
$$\kappa a^{(1)} + D_\omega b^{(1)} = \frac{-e}{m}[E_y \cos\alpha + E_z \sin\alpha] \qquad (4.1)$$

where we have introduced the following notation: $D_\omega = \omega_0^2 - \omega^2 - 2i\omega\gamma$.

To introduce a second-order nonlinear response, we suppose that the restoring force is not harmonic and reads for oscillator A

$$-m\omega_0^2 a - m\beta a^2 \qquad (4.2)$$

the same being true for oscillator B. Looking for the solutions oscillating at 2ω, we get the following set of equations:

$$D_{2\omega} a^{(2)} + \kappa b^{(2)} = -\beta a^{(1)2}$$
$$\kappa a^{(2)} + D_{2\omega} b^{(2)} = -\beta b^{(1)2} \qquad (4.3)$$

Solving eqs 4.1 and 4.3 allows us to straightforwardly calculate the various components of the hyperpolarizability tensor. Out of the 27 components, there are only six independent ones and three null ones. Expression of these components in the hypothesis that the electrostatic coupling is weak is given in the Appendix A. Once the hyperpolarizability is known, the surface susceptibility, $\chi^{(2)}$, is obtained by averaging over a uniform distribution of φ's, as expected for an isotropic surface. The angles θ and ψ are supposed fixed. To begin with, we recover the expected results for the C_∞ symmetry of the problem: the only nonzero components of $\chi^{(2)}$ are 333, 311 = 322, 113 = 131 = 223 = 232, 123 = 132 = −213 = −231, the last four ones being characteristic of a chiral surface.[14] The expressions of the achiral components are complicated, but if we suppose that the coupling is weak, they can be all shown to vary as

$$\beta \frac{1}{D_\omega^2 D_{2\omega}}. \qquad (4.4)$$

We recover here the usual feature of the calculation of the second-order nonlinear response of a classical anharmonic oscillator:[20] these terms are nonzero whatever the (chiral or not) molecule, and they display resonances both at ω and 2ω. The unique independent chiral components vary as

$$\chi^{(2)}_{123} \propto \beta\kappa \frac{D_{2\omega} - D_\omega}{D_\omega^3 D_{2\omega}^2} \qquad (4.5)$$

Complete introduction of the coupling leads to more involved, but not dramatically different, expressions. Several comments may be done at this point. First of all, one sees that $\chi^{(2)}_{123}$ depends on the coupling factor, κ. If there is no coupling, the molecule is no longer optically active and the chiral susceptibility vanishes. Furthermore, far from resonances, $\chi^{(2)}_{123}$ goes to zero. This is not true for the achiral components. This is to be traced back to Kleinmann symmetry, which states that far from resonances, one can interchange the subscripts 1, 2, and 3 without changing the susceptibility.[14] This cancellation far from resonance is therefore much more general than this particular calculation.

B. Model of the ORD-SHR in the Tröger Base. Now that we have the expressions of the surface susceptibility tensor, there is no problem to calculate the nonlinear polarization, $\mathbf{P}^{(2)}(2\omega) = \epsilon_0\chi^{(2)}\mathbf{E}^2(\omega)$, and the SH electric field radiated in the $\mathbf{n}$ direction, $\mathbf{E}(2\omega) \propto \mathbf{n} \times (\mathbf{P} \times \mathbf{n})$,[14] and to deduce the expressions of the f_p and f_s coefficients. Once these latter are obtained, the SH rotation angle is given by eqs 2.7 and 2.8. The total expressions are of course quite involved but easy to handle with the help of the Mathematica software to obtain the desired results. The crucial point is rather the choice of the parameters. To account for our experimental results with our model calculation, we need to know three sets of parameters: the absorption band characteristics (ω_0 and γ), the geometrical characteristics (the angles θ and ψ and the angle α), and the coupling strength (κ). The first set of parameters may be directly estimated from the experimental absorption curve. From the geometry of the molecule, we estimate $\alpha \approx 30°$ (Note that this angle corresponds to the orientation of the *dipole moments* and not of the acridine axes). The values of θ and ψ deal with the way the molecules are fixed on the surface. It seems reasonable to assume that the two terminal amine groups will lay on the surface because the silica substrate undergoes a hydrophilic treatment prior to the deposition of the molecules. This hypothesis fixes a relationship between θ and ψ but not their absolute values because we do not have any information about the tilt angle of the molecules. However, the absolute values are not important, and we have checked that the final result is only very weakly dependent on them. We have thus chosen $\theta = 30°$ and $\psi = -60°$. The choice of the coupling parameter is, on the other hand, much more critical. From geometrical considerations, developed in Appendix B, we estimate $\kappa/\omega_0^2 \approx 0.35$. This corresponds to a very large interaction between the

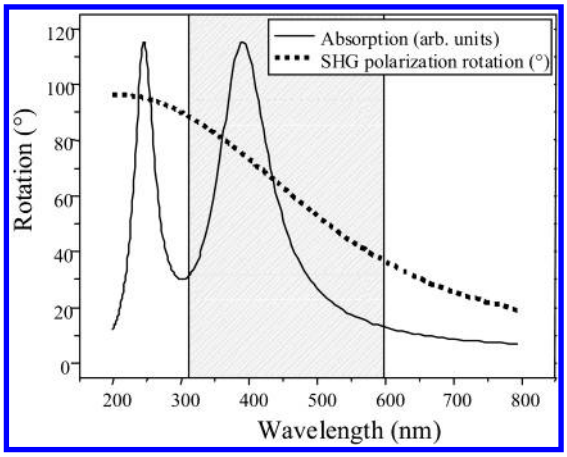

Figure 5. Results of the model calculation: (···) SHR rotation angle (in deg); (—) absorption spectrum (in arbitrary units). The grayed protion corresponds to the experiment (cf Figure 2).

two acridines, which is in agreement with the single-signed circular dichroism in this region.[17] This description should, however, not been taken for more than a qualitative description of the circular dichroism structure because the absorption band in the visible is in reality composed of many transitions.[17] It nevertheless allows us to describe the behavior of the SH polarization as a function of the fundamental wavelength fairly well.

With the help of the above-defined parameters, we obtain the absorption and the SH rotation as shown in Figure 5. The grayed portion is to be compared with the experimental results displayed in Figure 2. One can see that the agreement is very correct. The overall shape of the curves is qualitatively good, and the order of magnitude of the rotation angle is quite quantitative. We also recover the fact that the SH rotation angle δ_m does not show any special feature when the SH photon energy is in resonance with the absorption band but only regularly increases. The resonance effect in f_p and f_s does exist but is washed out when considering tan δ_m, which depends on the ratio of these parameters. In fact, a resonance structure is expected when $|f_p|^2 = |f_s|^2$ in the tan function, but it does not show up in the rotation angle. In Figure 5, one can see the two peaks that correspond to the lifting of the degeneracy of the two oscillators due to the coupling. Because the coupling is strong, the shift is very important and the high-energy peak is expected to be hidden by strong transitions lying in the UV.[17]

V. Conclusion

In this article, we have focused our attention on the polarization rotation in second harmonic generation from an isotropic surface of chiral molecules. We have first carefully analyzed the dependence of the rotation angles with the various parameters, emphasizing that this measurement is only relevant for chiral molecules of which the optical activity is of electric origin. We have then brought an experimental evidence by synthesizing an acridine-substituted Tröger base. The presence of the two acridines arranged in a noncentrosymmetrical manner ensures the electric origin of the optical activity. With this molecule, we have achieved a very strong rotation (up to 66°) in accordance with our expectations. We have measured this rotation as a function of the wavelength for a frequency range spanning the absorption band and observed a continuous increase of the angle. Development of a model calculation based on the Kuhn model with coupled anharmonic oscillators has allowed us to reproduce satisfactorily the experimental results.

Appendix A: Hyperpolarizability Tensor

From the eqs 4.1 and 4.3, we calculate the various components of the hyperpolarizability tensor:

$$\beta^{eee}_{xxx} = \beta^{eee}_{yyy} = \frac{\beta e^3 \cos^3 \alpha}{\epsilon_0 m^2 D_\omega{}^2 D_{2\omega}} \tag{A1}$$

$$\beta^{eee}_{xxy} = \beta^{eee}_{xyx} = \beta^{eee}_{yxy} = \beta^{eee}_{yyx} = -\frac{\beta e^3 \kappa \cos^3 \alpha}{\epsilon_0 m^2 D_\omega{}^3 D_{2\omega}} \tag{A2}$$

$$\beta^{eee}_{xxz} = \beta^{eee}_{xzx} = -\beta^{eee}_{yyz} = -\beta^{eee}_{yzy} = \beta^{eee}_{zxx} = -\beta^{eee}_{zyy} = -\frac{\beta e^3 \cos^2 \alpha \sin \alpha}{\epsilon_0 m^2 D_\omega{}^2 D_{2\omega}} \tag{A3}$$

$$\beta^{eee}_{xzz} = \beta^{eee}_{zxz} = \beta^{eee}_{zzx} = \beta^{eee}_{yzz} = \beta^{eee}_{zyz} = \beta^{eee}_{zzy} = \frac{\beta e^3 \cos \alpha \sin^2 \alpha}{\epsilon_0 m^2 D_\omega{}^2 D_{2\omega}} \tag{A4}$$

$$\beta^{eee}_{xyy} = \beta^{eee}_{yxx} = -\frac{\beta e^3 \kappa \cos^3 \alpha}{\epsilon_0 m^2 D_\omega{}^2 D_{2\omega}{}^2} \tag{A5}$$

$$\beta^{eee}_{xyz} = \beta^{eee}_{xzy} = -\beta^{eee}_{yxz} = -\beta^{eee}_{yzx} = \frac{\beta e^3 \kappa \cos^2 \alpha \sin \alpha}{\epsilon_0 m^2 D_\omega{}^3 D_{2\omega}{}^2}(D_{2\omega} - D_\omega) \tag{A6}$$

$$\beta^{eee}_{zxy} = \beta^{eee}_{zyx} = \beta^{eee}_{zzz} = 0 \tag{A7}$$

At this point, it is worth commenting on the choice of the molecular framework. The final expression of the susceptibility tensor is of course independent of the choice of the molecular framework, and one can freely determine the more appropriate one. The Tröger base has a C_2 symmetry axis perpendicular to its methylene bridge. This corresponds in our model to the $x-y$ bisector. At first sight, it would seem better to choose a molecular framework involving this symmetry axis as the y-axis. By doing so, we would reduce the number of nonzero components to 8,[21] whereas we have 24 nonzero components. However, the choice of our framework matches very well the molecule geometry and allows us to have a better approach of the chirality of the molecule. Indeed, considering the above equations, one sees that there is a separation between *achiral* components (which do not depend on the coupling parameter κ) and *chiral* ones (which vanish if the coupling vanishes). The components that depend on κ are those for which the two space directions x and y come into play. This is understandable because only the components probing these two space directions will be sensitive to the coupling and thus to the chirality of the molecule. This would be no longer true with another framework.

Appendix B: Coupling Parameter

The coupling between the two oscillators is primarily an electrostatic coupling. The corresponding energy is given by[16]

$$V = \frac{e^2}{4\pi\epsilon_0} \frac{\mathbf{r}_a \mathbf{r}_b - 3(\hat{\mathbf{R}}_{ab} \cdot \mathbf{r}_a)(\hat{\mathbf{R}}_{ab} \cdot \mathbf{r}_b)}{R_{ab}{}^3} \tag{B1}$$

where $\mathbf{r}_{a,b}$ is the elongation of the oscillators A and B, and $\mathbf{R}_{ab}$ is the vector joining the center of the two oscillators, the circumflex sign denoting the corresponding unit vector. Noting D_0, the position of the center of the oscillators with respect to the z axis, we calculate $R_{ab}^2 = 2D_0^2 \cos^2 \alpha + d^2$ and

$$V = -\frac{e^2}{4\pi\epsilon_0}\frac{ab}{R_{ab}^3}\left(\sin^2 \alpha + 3\frac{D_0^2 \cos^4 \alpha - d^2 \sin^2 \alpha}{R_{ab}^2}\right) \quad \text{(B2)}$$

Taking $d = 1$ Å and $D_0 = 2$ Å, we calculate $V = 14ab$ J which we obtain $m\kappa = 14$ J/m^2. On the other hand, $m\omega_0^2$ can be estimated to 40 J/m^2, and finally, we obtain

$$\frac{\kappa}{\omega_0^2} \approx 0.35 \quad \text{(B3)}$$

This estimation is of course very crude. It nevertheless shows that the coupling estimated from geometrical arguments is compatible with our experimental findings.

References and Notes

(1) Petralli-Mallow, T.; Wong, T. M.; Byers, J. D.; Yee, H. I.; Hicks J. M. *J. Phys. Chem.* **1993**, *97*, 1383.

(2) Kauranen, M.; Verbiest, T.; Maki, J. J.; Persoons, A. *J. Chem. Phys.* **1994**, *101*, 8193.

(3) Schanne-Klein, M. C.; Hache, F.; Roy, A.; Flytzanis, C.; Payrastre, C. *J. Chem. Phys.* **1998**, *108*, 9436.

(4) Fischer, P.; Buckingham, A. D. *J. Opt. Soc. Am. B* **1998**, *15*, 2951.

(5) Angeluts, A. A.; Balakin, A. V.; Boucher, D.; Il'ina, I. G.; Koroteev, N. I.; Masselin, P.; Mikhalev, O. A.; Pakulev, A. V.; Fertein, E.; Shkurinov, A. P. *Opt. Spectrosc.* **1999**, *87*, 151.

(6) Petralli-Mallow, T. P.; Plant, A. L.; Lewis, M. L.; Hicks, J. M. *Langmuir* **2000**, *16*, 5960.

(7) Verbiest, T.; Kauranen, M.; Van Rompaey, Y.; Persoons, A. *Phys. Rev. Lett.* **1996**, *77*, 1456.

(8) Simpson, G. J. *J. Chem. Phys.* **2002**, *117*, 3398.

(9) Kauranen, M.; Maki, J. J.; Verbiest, T.; Van Elshocht, S.; Persoons, A. *Phys. Rev. B* **1997**, *55*, R1985.

(10) Felderhof, B. U.; Bratz, A.; Marowsky, G.; Roders, O.; Sieverdes, F. *J. Opt. Soc. Am. B* **1993**, *10*, 1824.

(11) Byers, J. D.; Yee, H.; Hicks, J. M. *J. Chem. Phys.* **1994**, *101*, 6233.

(12) Schanne-Klein, M. C.; Hache, F.; Brotin, T.; Andraud, C.; Collet, A. *Chem. Phys. Lett.* **2001**, *338*, 159.

(13) Kauranen, M.; Verbiest, T.; Persoons, A. *J. Mod. Opt.* **1998**, *45*, 403.

(14) Hache, F.; Mesnil, H.; Schanne-Klein, M. C. *J. Chem. Phys.* **2001**, *115*, 6707.

(15) Schanne-Klein, M. C.; Boulesteix, T.; Hache, F.; Alexandre, M.; Lemercier, G.; Andraud, C. *Chem. Phys. Lett.* **2002**, *362*, 103.

(16) Rodger, A.; Norden, B. *Circular Dichroism and Linear Dichroism*; Oxford University Press: Oxford, U.K., 1997.

(17) Tatibouët, A.; Demeunynck, M.; Andraud, C.; Collet, A.; Lhomme, J. *Chem. Commun.* **1999**, 161.

(18) Kuhn, W. *Z. Phys. Chem. Abt. B* **1929**, *14*, 29.

(19) Han, S. H.; Ji, N.; Belkin, M. A.; Shen, Y. R. *Phys. Rev. B* **2002**, *66*, 165415.

(20) Boyd, R. W. *Nonlinear Optics*; Academic Press: Boston, MA, 1992; p 21.

(21) Butcher, P. N.; Cotter, D. *The elements of nonlinear optics*; Cambridge University Press: Cambridge, U.K., 1990; p 303.